Desalination and Water Treatment
www.deswater.com

doi: 10.5004/dwt.2021.27432

230 (2021) 331–345
August

Electrochemical behaviors of waste steel container as electrodes for removal of Acid Red 18 dye in water through electrocoagulation process

Amri Nurulhuda[a,b], Ismail Suzylawati[a], Azha Syahida Farhan[a], Abdullah Ahmad Zuhairi[a,*]

[a]*School of Chemical Engineering, Universiti Sains Malaysia, Engineering Campus, 14300 Nibong Tebal, Pulau Pinang, Malaysia, Tel. +604-599 6411; Fax: +604-599 5908; emails: chzuhairi@usm.my (A.A. Zuhairi), nurulhuda.amri@gmail.com (A. Nurulhuda), chsuzy@usm.my (I. Suzylawati), syahidafarhan1989@gmail.com (A.S. Farhan)*
[b]*Faculty of Chemical Engineering, Universiti Teknologi MARA, Cawangan Pulau Pinang, Kampus Permatang Pauh, 13500 Permatang Pauh, Pulau Pinang, Malaysia*

Received 22 January 2021; Accepted 15 May 2021

ABSTRACT

Solid wastes are one of the major environmental problems and creative utilization could hold the key to the solution. An attempt was made in this study to transform waste from steel containers (WSC) into efficient electrodes for the removal of Acid Red 18 dye from water through an electrocoagulation (EC) process. A 1.1 L batch monopolar EC cell with two pre-treated WSC electrode plates connected to an external DC power supply was used. Effects of current density (5–25 mA/cm^2), initial pH (3–11), initial dye concentration (50–250 mg/L), NaCl dosage (0.5–4.0 g/L) and inter-electrode distance (IED) (0.5–2.5 cm) were demonstrated. The best removal of 97.0% ± 1.0% with low sludge production was obtained at a current density of 10 mA/cm^2, a pH of 6.8 (original pH of dye), an initial dye concentration of 100 mg/L, a NaCl dosage of 2 g/L, an IED of 0.5 cm and a reaction time of 5 min. The electrical energy consumption and cost of operation were estimated at 0.3717 kWh/m^3 and US$ 0.9738/m^3, respectively. Thus, the WSC electrodes could serve as an economical remedial option for the electrocoagulation treatment of dye-containing wastewater while addressing the solid waste problem.

Keywords: Electrocoagulation; Waste steel container; Acid Red 18 dye; Electrochemical process behavior; Sludge; Mechanism

1. Introduction

Rapid economic development and population growth cause a surge of solid wastes generation that is creating severe environmental issues. Steel container wastes (WSC) are ferrous metal wastes that significantly contribute to the generated solid wastes because of the extensive use for packaging various products. This stems from their excellent anti-corrosion property as well as strength in withstanding shipment and storage [1]. Between September 2011 to September 2012, 2.4% of the total solid wastes generated in Malaysian was contributed by ferrous metal wastes whereby 211 metric tonnes of this waste ended up in landfills daily [2]. The World Steel Association reported that approximately 86 million tonnes of scrap steel were produced in 2016 alone with only 70% of the scrap steel successfully recycled [3]. As such, the creative utilization of the currently unrecovered portion of this waste is deemed necessary.

Steel wastes could be transformed into various products to minimize their environmental impacts such as electrocatalysts [1] and nanocomposite catalysts [3]. According to Devi et al. [1], tin-plated steel wastes that were successfully transformed into iron nanosheets that could

---

* Corresponding author.

be used in the energy conversion field relied on their electrocatalytic activity. Another possibility in reutilizing metal wastes is by converting them to electrodes for the electrocoagulation (EC) process to be used in wastewater treatment. The presence of high Fe contents that is responsible for their excellent conductive property allows them to function as effective electrodes during the EC process [4].

EC process is an emerging technology in wastewater treatment and it combines the benefits of electrochemistry, coagulation, and flotation to remove numerous persistent pollutants efficiently [4]. Recently, eco-friendly renewable energy alternatives such as solar photovoltaic and wind turbines have been proposed for use in the EC process to improve their sustainability, particularly in remote areas where the electricity grid is unavailable [5,6]. For EC application, Al and Fe have been identified as the most effective electrode elements due to high electro-dissolution rates, high charge valence, readily available, non-toxic, and low cost [7]. A high anode dissolution rate with greater charge valence metal-ionic coagulants are essential in boosting the EC process due to more substantial electrical double-layer compression that enhances the coagulation process [8]. Insoluble $Al(OH)_3$ or $Fe(OH)_3$ species that are formed through the anodic dissolution will act as the main coagulant for removing the pollutants. Nonetheless, there are two possible reaction mechanisms involved when Fe or steel electrode is used as given in Eqs. (1)–(8) [9,10]. It is anticipated that the main Fe species in the system is Fe(III) as Fe(II) is not stable can be easily oxidized to Fe(III).

Mechanism 1:

Anode:

$$\mathrm{Fe(s)} \rightarrow \mathrm{Fe^{2+}(aq)} + 2\mathrm{e^-} \tag{1}$$

$$\mathrm{Fe^{2+}(aq)} + 2\mathrm{OH^-(aq)} \rightarrow \mathrm{Fe(OH)_2(s)} \tag{2}$$

Cathode:

$$2\mathrm{H_2O} + 2\mathrm{e^-} \rightarrow \mathrm{H_2(g)} + 2\mathrm{OH^-(aq)} \tag{3}$$

Overall reaction:

$$\mathrm{Fe(s)} + 2\mathrm{H_2O} \rightarrow \mathrm{Fe(OH)_2(s)} + \mathrm{H_2(g)} \tag{4}$$

Mechanism 2:

Anode:

$$4\mathrm{Fe(s)} \rightarrow 4\mathrm{Fe^{2+}(aq)} + 8\mathrm{e^-} \tag{5}$$

$$4\mathrm{Fe^{2+}(aq)} + 10\mathrm{H_2O} + \mathrm{O_2(g)} \rightarrow 4\mathrm{Fe(OH)_3(s)} + 8\mathrm{H^+(aq)} \tag{6}$$

Cathode:

$$8\mathrm{H^+(aq)} + 8\mathrm{e^-} \rightarrow 4\mathrm{H_2(g)} \tag{7}$$

Overall reaction:

$$4\mathrm{Fe(s)} + 10\mathrm{H_2O} + \mathrm{O_2(g)} \rightarrow 4\mathrm{Fe(OH)_3(s)} + 4\mathrm{H_2(g)} \tag{8}$$

The use of Fe or steel electrodes for the EC process has been explored in recent years. The areas of focus included the understanding of the relevant mechanism, the influences of operating parameters (current density, initial pH, and reaction time), and the applicability in treating textile industry effluents [11–14]. Azo dyes which represent over 70% of all commercially produced dyes are widely used in the textile industry [15]. They have one or more azo groups (–N=N–) that are mostly substituted by sulfonate groups. This results in intense color, high water solubility and stability under sunlight, and resistance to degradation under conventional biological treatment [10,12,16]. Due to this reason, many studies have primarily focused on the treatment of azo dye-containing wastewater using various electrochemical methods [17].

Azarian et al. [18] conducted a batch monopolar EC process using both pure Al and Fe electrodes to eliminate synthetic Acid Red 18 (AR18) which is a model pollutant of azo dyes. They observed that the Fe electrode demonstrated higher color and chemical oxygen demand (COD) removal efficiencies of up to 99.5% and 59.0%, respectively, with lower energy consumption than the Al electrode. Similarly, Malakootian and Moridi [15] investigated the efficiency of an electro-Fenton process in eliminating AR18 dye from an aqueous solution using two plain Fe electrodes, with the addition of H_2O_2 as an oxidizing agent. Their study revealed that the maximum removal efficiency for AR18 dye under optimal process conditions was 99.9% ± 0.2% and 90.5% ± 1.7%, respectively. The conditions stipulated were a voltage of 30 V, a pH of 3, an electrolyte concentration of 100 mg/L, an H_2O_2 concentration of 1 mL/L, and an electrode distance of 1 cm. These results further supported the argument that the Fe electrode was essential in removing dye compounds from synthetic or industrial wastewaters. However, commercial Fe electrodes were commonly used for dye removal in those studies.

Theoretically speaking, different elemental alloying elements can influence the corrosion resistance by altering the phase structure and elemental segregation which consequently affects the passive film properties as well as the dissolution kinetics during the EC process [19,20]. Thus, it is critical to investigate the performance of the proposed WSC electrode for wastewater treatment, as it may contain different alloying elements than those of the commercial Fe electrode reported in the literature, resulting in a different pollutant removal efficiency. The utilization of WSC material as an electrode for such application has yet to be sufficiently investigated so far. Furthermore, the best experimental conditions for the EC process using WSC electrodes should also be examined because they have a significant effect on dye removal efficiency and mechanism, energy consumption, sludge production, as well as residual Fe ions in treated water.

Therefore, an attempt was made in this work to demonstrate the applicability of WSC as an alternative to commercial steel-based electrodes for the removal of AR18 dye through an EC process. This new approach could significantly reduce the cost to replace the electrodes after the EC process. A pretreatment step was first required to eliminate the outer and inner coating layers of the WSC to be transformed into EC electrodes. The physical appearances and elemental compositions before and after the treatment were closely examined to check for the suitability of the pretreatment method for the decoating process. The subsequent study on the effect of operational parameters was carried out in a batch EC process to demonstrate the process behaviors in the removal of AR18 dye. Understandings on the roles of electrochemical parameters such as current density and inter-electrode distance were particularly attempted. The sludge was also characterized to identify the dominant AR18 dye removal mechanism considering the role of H_2 bubbles in the formation of flocs scum. At the same time, the residual Fe content in the effluent was also analyzed to ensure compliance with the industrial effluent discharge standard in Malaysia.

2. Materials and methods

2.1. Chemicals

All chemicals used in this study, that is, AR18 dye (>99% purity), hydrochloric acid (HCl) (37% purity), sulfuric acid (H_2SO_4) (95%–98% purity), sodium hydroxide (NaOH) and sodium chloride (NaCl) were of analytical grade and purchased from Merck (USA). The sandpaper used for the decoating of the waste was a P180 SiC Paper (SeaHawk, Malaysia).

2.2. Pretreatment of WSC electrodes

The WSC sample was collected from a student hostel in Universiti Sains Malaysia. The WSC was used in its original form and was first cut into T-shaped pieces with specific dimensions as shown in Fig. 1 [21]. In order to eliminate the coating layers on both outer and inner walls, they were pretreated by sanding using a sandpaper before rinsing with deionized water. The WSC was then air-dried and ready to be characterized as well as used as electrodes in the batch EC experiment.

2.3. Batch EC system

The batch monopolar EC experiments were carried out in a 1.1 L rectangular reactor as schematically shown in Fig. 2. Two pieces of WSC electrodes were placed at the center of the cell in such a way that an area of 6 cm × 7 cm of each electrode (42 cm^2) was dipped into the solution. The total surface area of both sides of the anode was 84 cm^2. As the thickness of the electrode was lower than 0.5 mm, the contribution of the surface area of the edges of the electrodes towards the calculation of the current density was negligible. 800 mL of the dye solution was then fed into the EC cell. During the EC process, the solution was continuously stirred with a magnetic stirrer (Topolino, IKA). All the experiments were carried out at a room temperature of 25°C ± 1°C. The required energy throughout the experiment was supplied by a DC power supply (Dazheng PS-305D, 0–5 A, 0–30 V). Samples of the treated wastewater were then taken at different process times and filtered through a Whatman Filter Paper before the measurement of color. After filtration, the sludge was collected and dried overnight in an oven at 105°C for characterization analyses.

The AR18 dye removal efficiency is calculated using Eq. (9):

$$\text{Removal Efficiency},\% = \frac{C_0 - C_t}{C_0} \times 100\% \quad (9)$$

where C_0 = the initial dye concentration (mg/L); C_t = dye concentration at a time, t (mg/L).

Each of the EC experiments was conducted in duplicate and the average dye removal efficiency was calculated to ensure the accuracy and reproducibility of the experimental data with variations within ±5% of standard deviation (SD). The SD value was determined using Eq. (10). The variations of the experimental data are represented by the error bars marked in the plotted graphs.

$$\text{SD} = \sqrt{\frac{1}{n-1}\sum_{i=1}^{n}\left(x_i - \bar{x}\right)^2} \quad (10)$$

where x_i = the dye removal efficiency (%); $\bar{x}$ = the average of dye removal efficiency (%); n = the number of experimental data points.

2.4. Electrical energy consumption

The cost of the operation is usually estimated based on the amount of energy, the mass of the electrode, and the

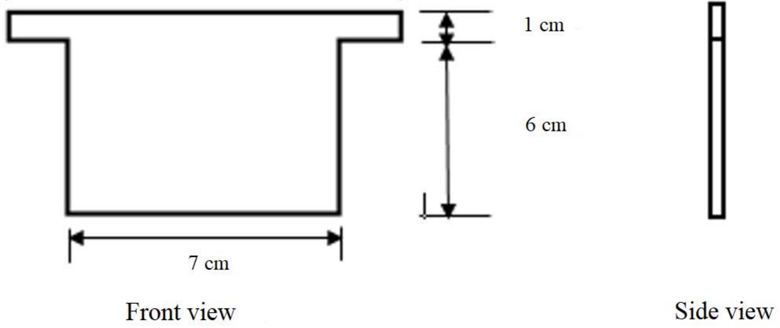

Fig. 1. Specific dimensions of the WSC electrodes.

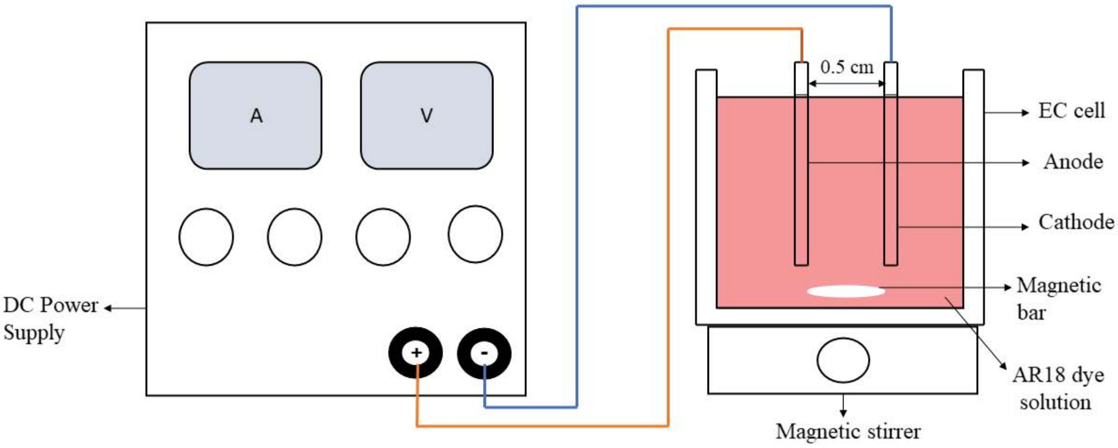

Fig. 2. Schematic diagram of the EC experimental set-up.

chemical consumption used during the EC process [22]. For the sake of simplicity, the cost for electrode consumption was neglected in this study since the electrodes used were made from waste material. Furthermore, the preparation of the electrode material also involved physical treatment that was performed manually. The electrical energy consumption (EEC) and operating cost are determined using Eqs. (11) and (12), respectively.

$$\text{EEC},\left(\text{kWh/m}^3\right)=\frac{V\times I\times t}{v} \tag{11}$$

where V = the applied voltage (V); I = the required current (A); t = time (h); v = volume of dye solution (m^3).

$$\text{Operating cost},\left(\$\right)=a\times\text{EEC}+b\times\text{CC} \tag{12}$$

where a = the electrical city price (US$/kWh); b = the chemical unit price (US$/kg); EEC = electrical energy consumption (kWh/m^3); CC = chemical consumption (kg/m^3).

According to the rates and tariffs in Malaysia throughout January 2021, the electrical cost was at US$ 0.091/kWh [23]. Meanwhile, the price for NaCl was at US$ 0.47/kg.

2.5. Analytical methods

The main concern of this study is to examine the removal efficiency of the original substance (AR18 dye) not the possible intermediates formed during the EC process. Thus, the concentration of the samples was determined using a double beam UV-visible spectrophotometer (UV-1800, Shimadzu, Japan) based on the absorbance values at a maximum wavelength (λ_{max}) of 507 nm for the AR18 dye. The surface morphology and the elemental composition of WSC floc after the EC process was examined using a scanning electron microscope (SEM) equipped with an energy-dispersive X-ray spectroscopy (EDX) facility (Quanta 450 FEG, FEI, Netherlands) operated at an accelerating voltage of 5 kV. The functional groups of the AR18 dye and WSC floc were identified using a Fourier-transform infrared spectrophotometer (IRPrestige-21, Shimadzu, Japan). The concentration of Fe ions in the treated water was analyzed using an inductively coupled plasma-optical emission spectrometer (ICP-OES) (iCAP 7600, Thermo Scientific, USA). The conductivity and pH of the solution were measured using a conductivity meter (HI98192, Hanna Instrument, Romania) and a pH meter (Eutech pH 2700, Thermo Scientific, Singapore), respectively.

3. Results and discussion

3.1. Effect of the pretreatment method on WSC surface

In this study, sandpaper was used to remove the coating layers on both the outer and inner walls of the WSC. Based on Fig. 3, the paint coating on the WSC electrodes could be effectively removed by this method. On the other hand, the effect of this pretreatment method on the inner coating of WSC could not be examined with naked eyes due to the transparent coating inside the WSC materials. Thus, the inner surfaces of WSC after the pretreatment were characterized using SEM-EDX analyzer, which identified the surface morphology and elemental composition before and after each pretreatment, as also given in Fig. 3. It illustrates the surface morphology of the inner coatings on WSC. The surface of the WSC electrode before pretreatment was relatively smooth to indicate that the inner coating was homogenous with an even surface. From the EDX results, tin (Sn) was found to be the predominant component of the coating layer, along with iron (Fe) and carbon (C), with a composition of 50.6%, 43.0%, and 6.5%, respectively. This Sn coating was essential to WSC to prevent the corrosion of the steel that can contaminate food through the dissolved metals. Furthermore, the presence of carbon could be associated with the essential alloying element of Fe in making the steel.

Fig. 3 also shows the surface morphology of the inner WSC electrodes after the mechanical pretreatment, which was observed to have changed and became somewhat coarser due to the application of P180 SiC Paper in removing

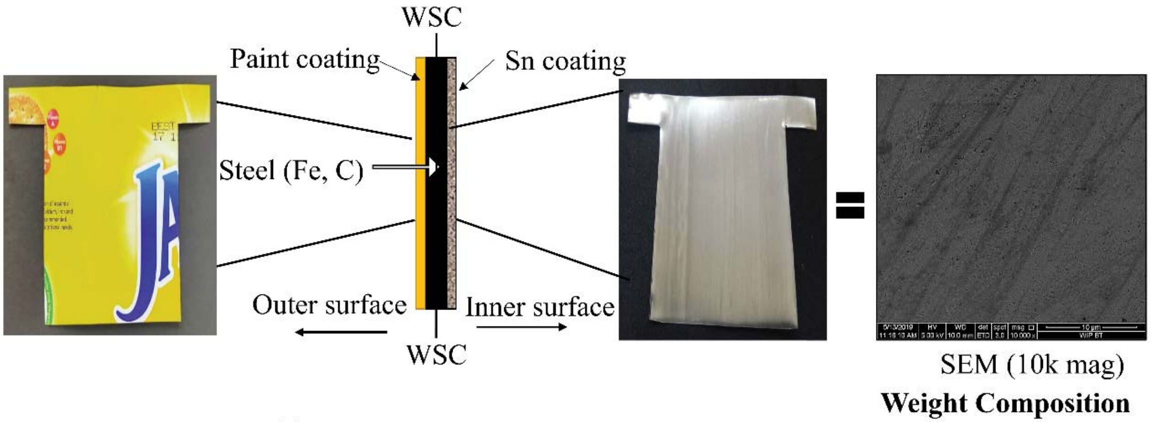

(a) WSC before pre-treatment

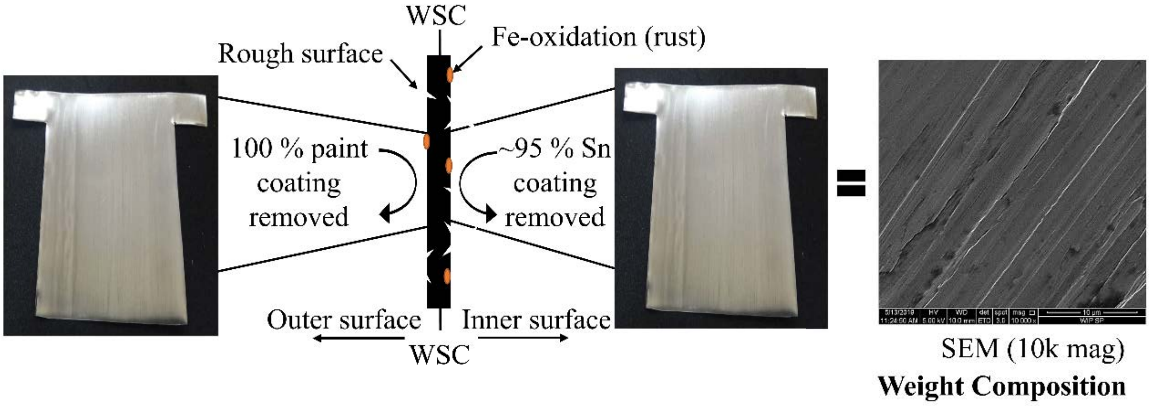

(b) Mechanical pre-treatment

Fig. 3. Effects of the mechanical pretreatment on the surface and elemental composition of the WSC electrode.

the surface coating. This method was considered beneficial for the WSC materials to reduce the Sn composition from 50.6% to 2.7%. Though a small amount of Sn could still be detected after the mechanical pretreatment, the high percentage of Sn removal of 94.6% suggested that the mechanical pretreatment was still adequate to be applied for eliminating most of the surface coating. As a result, the Fe and C contents increased by about 40.0% and 3.48%, respectively, when the Sn layer was removed after the pretreatment. Therefore, the mechanical pretreatment was found to be sufficiently effective in removing both the inner and outer coatings of WSC.

3.2. *Effect of operating parameters on decolorization of AR18 dye*

3.2.1. *Effect of current density*

Current density is one of the most critical parameters in controlling the electrochemical reaction rate such as the coagulant production rate and the size of the bubble generated that can affect the growth of flocs in the EC process. It is a measure of the current per area of the electrode, which determines the number of metal ions released from the electrodes. In this study, the effect of current density on the removal efficiency of AR18 dye was investigated by varying the current density between 5 to 25 mA/cm^2 at the original pH of the dye solution (pH 6.8). The initial dye concentration was fixed at 100 mg/L with a NaCl dosage of 2 g/L, an inter-electrode distance of 0.5 cm, and 10 min of reaction time.

Fig. 4a shows the influence of current density on the removal efficiency of AR18 dye against the reaction time. The results suggested that the removal of AR18 dye increased as the current density was increased. During the first 3 min of the reaction, the lowest AR18 dye removal of 28.8% was obtained at a minimum current density of 5 mA/cm^2. On the other hand, the highest AR18 removal of 96.4% was achieved at the maximum current density of 25 mA/cm^2. The higher efficiency in dye removal as the current density escalated was mainly due to the considerable amount of Fe ions dissolved from the electrodes, which was in agreement with Faraday's Law [24]. The release of cationic Fe ions from the electrode into the solution boosted the compression of the diffused double layer around the charged species. The destabilization of dye molecules due to charge neutralization then occurred to result in the agglomeration of flocs [12]. Higher current also meant more generation of H_2 microbubbles at the cathode to carry some of the flocs to the surface forming flocs scum. The formation of these metal hydroxide flocs with large surface

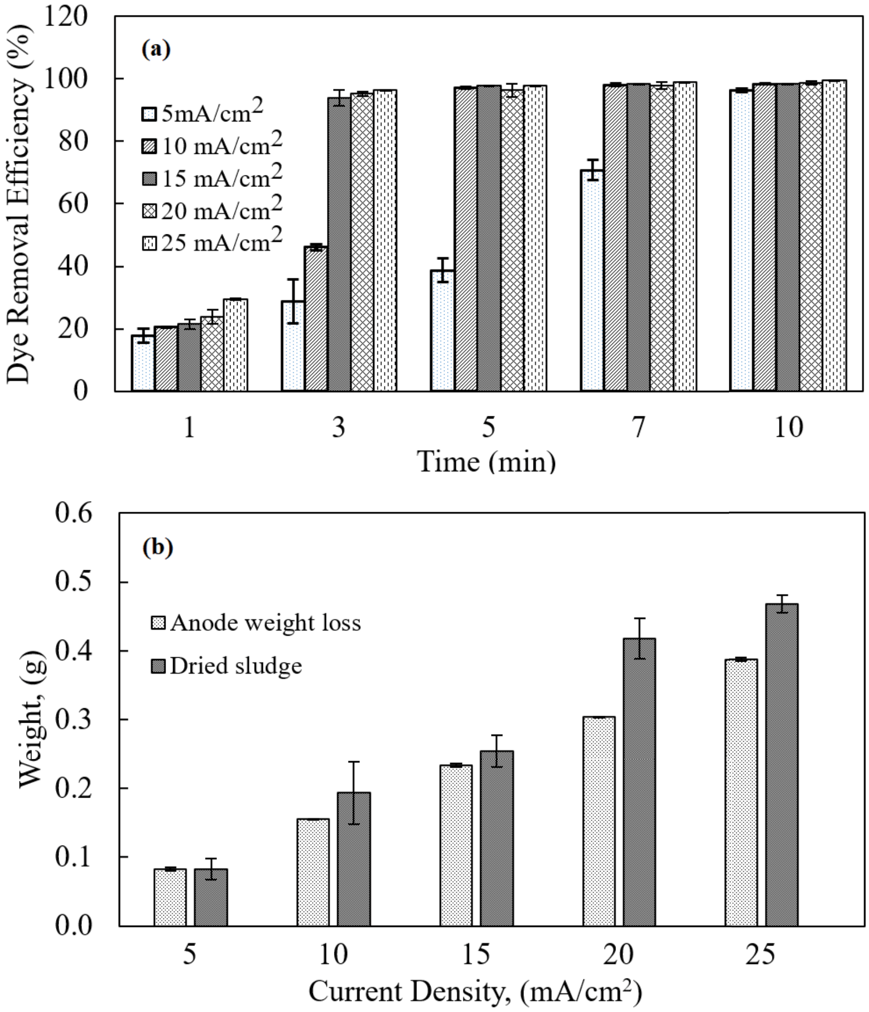

Fig. 4. Effects of current density on (a) dye removal efficiency and (b) anode weight loss and amount of dried sludge produced using WSC electrode. (Initial pH = 6.8; initial dye concentration = 100 mg/L; NaCl = 2 g/L; IED = 0.5 cm; time = 10 min).

areas allowed rapid adsorption of dye molecules. Moreover, higher current density was associated with the increase in the smaller size hydrogen bubbles that were produced at the cathode, leading to a higher dye removal by flocculation [25] and hydrogen floatation [26].

However, as the reaction time was increased to 5 min, there was no significant difference in the removal efficiency observed for the current density of 10–25 mA/cm^2, with the removal efficiency reaching up to around 97.0%. Further increase in the reaction time to 10 min resulted in a minimal increase of removal efficiencies at around 1%–2% for all current densities, except for the current density of 5 mA/cm^2. This observation concluded that the adsorption of dye molecules on the flocs was rapid only at the initial stage. After a specific time, the adsorption process progressive became constant [27]. The highest dye removal efficiency of 99.5% was achieved at a current density of 25 mA/cm^2 with a reaction time of 10 min.

In addition to the removal efficiency, current density also had a significant influence on the weight loss of the anode electrode and dried sludge production as illustrated in Fig. 4b. As the current density was increased from 5 to 25 mA/cm^2, both the weight loss of anode and dried sludge production was observed to progressively increase from 0.08 to 0.39 g and 0.08 and 0.47 g, respectively. Similar findings were reported by other researchers [25,28,29]. Hussin et al. [25] reported that high current density correspondingly resulted in high sludge production and also led to more passivation of the cathode because of the intensive hydroxide anion. Hydroxide anion was accountable for the formation of thick turbid sludge in the solution which further increased the applied voltage and the energy consumption.

Moreover, the increase in current density also contributed to an upsurge of weight loss of the anode that would shorten the lifetime and caused the electrode to be frequently replaced. Hence, a current density of 10 mA/cm^2 was selected for further studies because a high dye removal efficiency of 97.0% was demonstrated within 5 min of reaction time, as well as lower electrode consumption and dried sludge with reasonable energy consumption. A similar finding was reported by Ghalwa et al. [12] whereby the optimum current density was 10 mA/cm^2 with the percentage of dye and COD removal at 99.85% and 90.5%, respectively in 14 min of reaction time. In another study, Aleboyeh et al. [30] reported that the maximum AR15 dye removal of higher than 91% was obtained at 102 A/m^2 within only 4.47 min of reaction time.

3.2.2. Effect of pH

The initial pH of the water is known to have a considerable effect on the efficiency of pollutant removal in the EC process. Hence, the batch EC process was then performed to assess the effect of initial pH on dye removal efficiency. The change in pH within a range of 3 to 11, at a current density of 10 mA/cm^2, an initial dye concentration of 100 mg/L, a NaCl dosage of 2 g/L, an inter-electrode distance of 0.5 cm, and 10 min of reaction time was performed. The results for dye removal efficiency at different initial pH levels as a function of time are depicted in Fig. 5a. The significant effect of the initial pH can be clearly observed within the first 3 min of reaction time. In the first 1 min of reaction, the highest dye removal efficiency of 24.3% was attained with an initial pH of 3, followed by an initial pH of 6.8 at 20.7% of dye removal. These results proved that high removal efficiency was achieved at relatively acidic to neutral initial pH conditions (pH 3–6.8) due to the nature and quantity of the Fe species that were likely to be formed during the EC process.

The Fe ions released from the anode oxidation [Eqs. (1) and (5)] will produce monomeric ions, ferric hydroxo complexes, and various other polymers such as Fe^{3+}, $Fe(OH)^{2+}$, $Fe(OH)_2$, $Fe(H_2O)_6^{3+}$, $Fe(H_2O)_5OH^{2+}$, $Fe(H_2O)_4(OH)_2^{1+}$, $Fe_2(H_2O)_8(OH)_2^{4+}$ and $Fe_2(H_2O)_6(OH)_4^{2+}$, depending on the pH of the solution [24]. All these complex species have a higher tendency to polymerize at pH 3.5 to 7.0 and exist in the solution as a gelatinous suspension. In this study, these monomeric or polymeric cation species would interact and destabilize the dye pollutant effectively as AR18 dye molecules bore negative charges in the water. This charge neutralization would result in the coagulation of the dye to form relatively larger flocs.

It is noted in Fig. 5a that the runs with all the initial pH ended up with almost similar removal efficiencies of between 95% to 99% after 5 min of reaction. It was also found that the solution pH steadily increased during the process from the respective initial level to between 6 and 10 (Fig. 5b). This was directly associated with the formation of

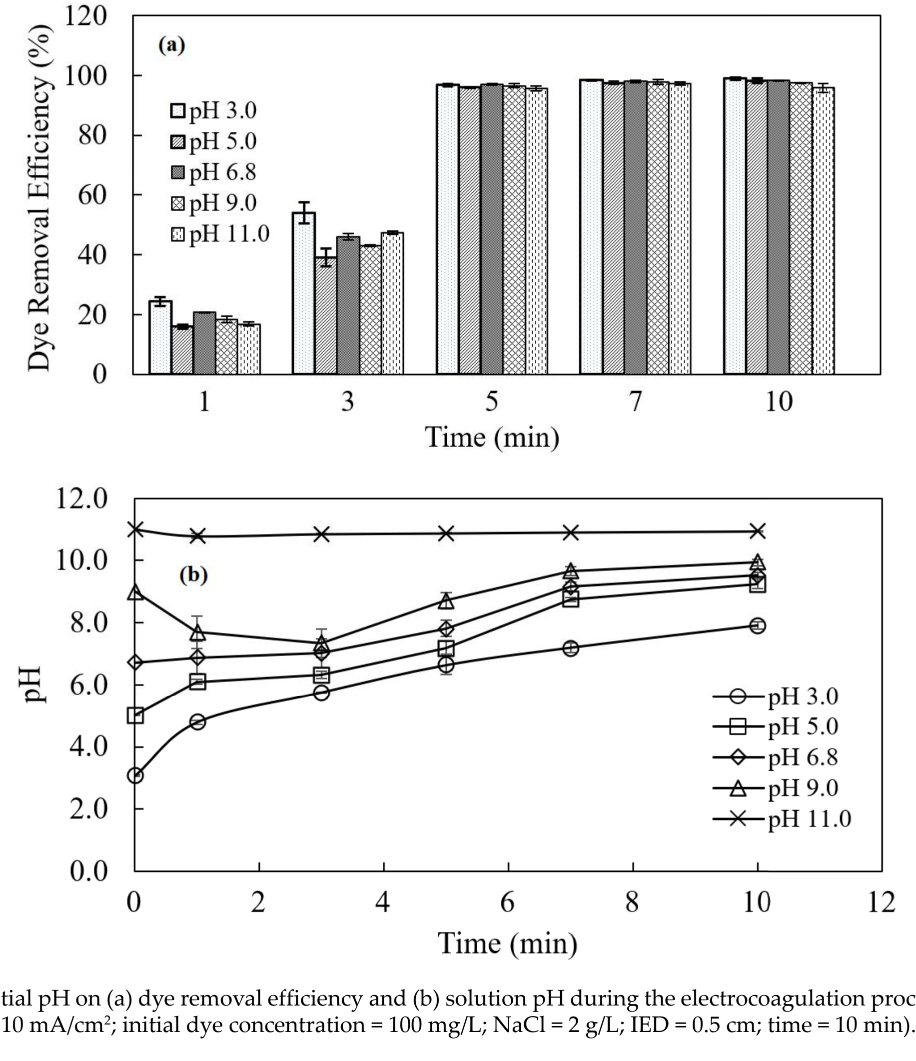

Fig. 5. Effects of initial pH on (a) dye removal efficiency and (b) solution pH during the electrocoagulation process by WSC electrode. (Current density = 10 mA/cm^2; initial dye concentration = 100 mg/L; NaCl = 2 g/L; IED = 0.5 cm; time = 10 min).

$^{-}$OH ions or the consumption of H^+ at the cathode as shown in Eqs. (3) and (7), respectively. The insoluble hydroxide species, that is, $Fe(OH)_3(s)$ that was generated from the EC process was stable within the range of pH condition (5–10), which further enhanced the adsorption of dye molecules onto $Fe(OH)_3(s)$ [11]. The Fe $(OH)_3$ and dye flocs were then removed from the solution through sedimentation or floatation by the bubbles.

The lowest removal efficiency of 95.8% was achieved in 10 min by the initial pH of 11. This result could be attributed to the formation of soluble Fe $(OH)_4^-$ species under the high alkaline condition which caused the coagulation process of the dye pollutant to be less effective due to the ionic repulsion between $Fe(OH)_4^-$ and the negatively charged dye molecules [4]. Therefore, the best initial pH to be applied in the EC process to remove AR18 dye was concluded to be at the original pH of 6.8. This finding was consistent with that reported by Jiménez et al. [31], who observed that pH values that were close to 7 (at pH of approximately around 7–8) were better for Fe electrocoagulation as the positively charged iron could be easily precipitated at this condition, which favored adsorption of anions. This finding could also mean that no pH adjustment of the solution was needed before the EC process. Similar results were also reported in several past studies that reported the best pH values obtained were at neutral conditions using pure aluminum and iron electrodes [18].

Furthermore, the pH of the solution was observed to change during the EC process, as presented in Fig. 5b. With an initial pH of 3, the pH of the treated effluent was found to increase up to 7.91. Meanwhile, the initial pH of 5.0, 6.8, and 9.0 resulted in increases in the pH of the solution to about 9.25, 9.52, and 9.95, respectively. The increase in overall solution pH can be described by the increase of hydroxide ions at the cathode during the EC process as water was reduced in the solution [14]. Conversely, at a high alkaline condition of pH 11, the final pH of the solution decreased slightly to 10.95 after the EC process. This occurrence can be explained based on the formation of hypochlorous acid in alkaline media [Eq. (14)]. Moreover, both $Fe(OH)_3$ and the release of H^+ ions [Eq. (6)] could also decrease the pH of the solution [32]. Similar observations on these changes of pH solution throughout the EC process had been established in other studies using other types of dyes and pure iron or aluminum electrodes [33,34]. This further justified that the EC process could also act as a pH neutralizer [35].

3.2.3. Effect of initial concentration

Fig. 6 shows the effect of initial dye concentration on dye removal efficiency using WSC electrodes. Overall, the removal efficiency exhibited a decreasing trend as the initial dye concentration was increased from 50 to 250 mg/L. This result was in line with the fact that at lower dye concentrations (50 and 100 mg/L), the number of iron hydroxide complexes produced was higher than the number of dye molecules. Hence, almost 97.0% of dye removal efficiency for both initial concentrations of 50 and 100 mg/L was obtained in only 5 min. On the contrary, the number of iron hydroxide complexes produced was lower than the dye molecules available at a higher range of initial dye concentrations of 150–250 mg/L. More amount of Fe hydroxide complexes was required for the decolorization of higher initial concentrations, with a larger surface area needed for the adsorption of dye molecules. A similar trend of removal efficiency at different initial concentrations was observed by Nandi and Patel [13] for the treatment of Brilliant Green Dye. They found that the dye removal efficiency decreased from 99.87% to 67.78% when the dye concentration was increased from 50 to 200 mg/L after 30 min of reaction. However, in this study, a near-complete dye removal was detected regardless of the initial concentration by prolonging the reaction time to 10 min. The number of iron hydroxide complexes generated, which increased with time, was deemed adequate to adsorb the highest initial dye concentration of 250 mg/L to result in 95.9% removal efficiency.

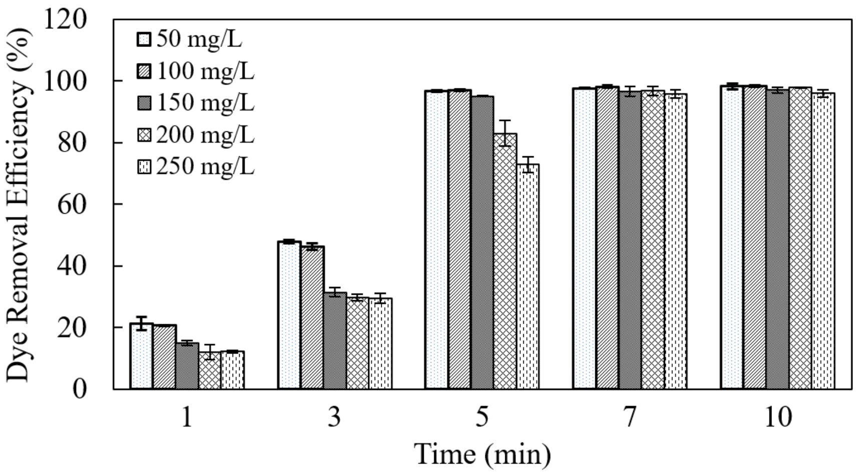

Fig. 6. Effects of initial dye concentration on dye removal efficiency by WSC electrode. (Current density = 10 mA/cm^2; initial pH = 6.8; NaCl = 2 g/L; IED = 0.5 cm; time = 10 min).

3.2.4. Effect of NaCl concentration

NaCl was chosen as a supporting electrolyte in this study due to the excellent electrolytic conductor that would enhance the pollutant removal as reported by some researchers [12,13]. It should be noted that NaCl is also extensively used in the textile industry to improve the adsorption of dye molecules on the fibers [36]. In this study, the influence of the NaCl dosage on the dye removal efficiency, the conductivity of solution as well as the required voltage for the process, was investigated. It was conducted by varying the NaCl dosage from 0.5 to 4.0 g/L while keeping other parameters constant.

The results for dye removal efficiency at various NaCl dosages are depicted in Fig. 7a. In the first 3 min of reaction, the dye removal efficiency appeared to escalate up to 46.1% as the NaCl dosage was increased from 0.5 to 2.0 g/L. However, the removal efficiency deteriorated to 39.8% and 37.3% when the NaCl dosages were higher, that is, at 3.0 and 4.0 g/L, respectively. A similar trend of dye removal performance with different dosages of NaCl has been reported earlier using aluminum electrodes [12]. Moreover, an increase in NaCl dosage up to 2.0 g/L significantly increased the conductivity of the dye solution while decreasing the cell resistance and voltage between the WSC electrodes. Consequently, the passage of electric current between the electrodes intensified to contribute to the upsurge of dissolution in the metal electrodes. Consequently, produced a higher amount of metallic hydroxide was produced to directly increase the dye removal efficiency [15,32].

The addition of sodium chloride can also produce hypochlorous acid [Eq. (14)] and hypochlorite ion [Eq. (15)]. These two types of oxidizers are formed at pH lower than 11. The presence of these species could oxidize the organic compounds of the dye as shown in the following reactions [37]:

$$2Cl^-(aq) - 2e^- \rightarrow Cl_2(g) \tag{13}$$

$$Cl_2(g) + H_2O(l) \rightarrow HOCl(aq) + Cl^- + H^+(aq) \tag{14}$$

$$HOCl(aq) \rightarrow OCl^-(aq) + H^+(aq) \tag{15}$$

Thus, an increase in the reaction time to 10 min was observed to cause no significant variation in the dye removal

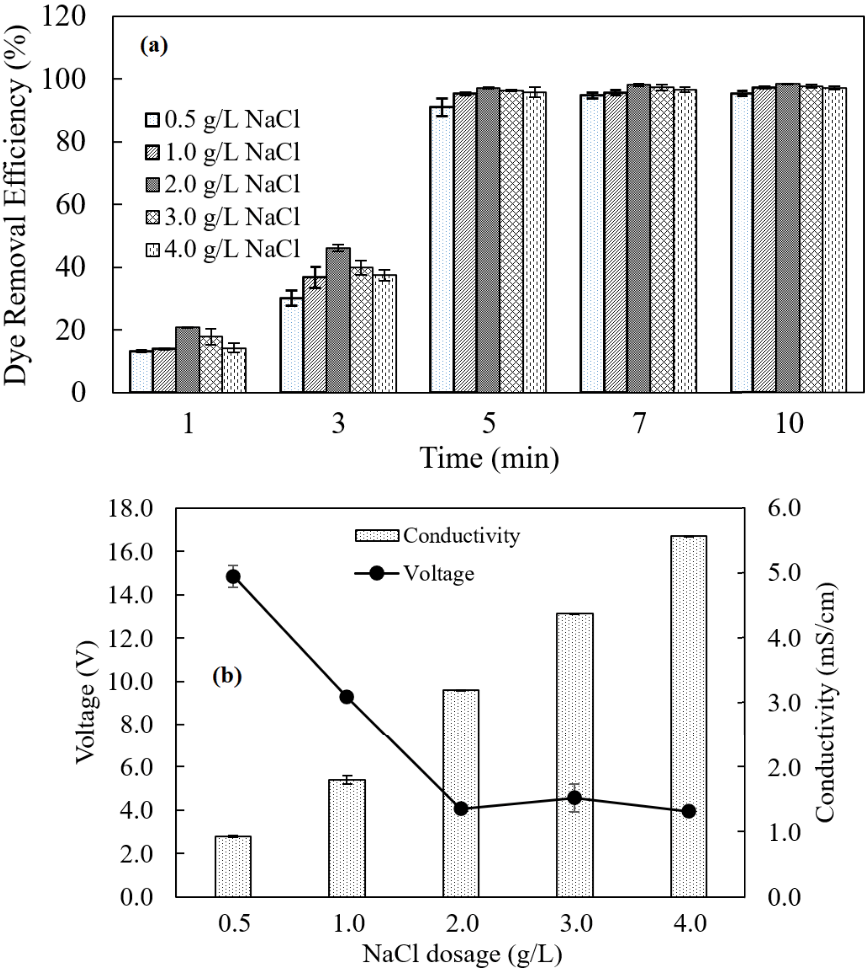

Fig. 7. Effects of NaCl dosage on (a) dye removal efficiency and (b) conductivity of the solution during the electrocoagulation by WSC electrode. (Current density = 10 mA/cm^2; initial pH = 6.8; initial dye concentration = 100 mg/L; IED = 0.5 cm; time = 10 min).

efficiency within the investigated range. All of the NaCl dosages achieved removals of up to 95.3 to 98.4% that were at par with those reported in previous studies [38]. However, the lower the NaCl dosage, the longer the WSC electrodes could last as a higher concentration of Cl^- promoted the occurrence of pitting corrosion phenomenon. It is a localized corrosion phenomenon that leads to small holes being formed on the surface of the electrode [39].

The significant effect of different NaCl dosages on the conductivity of the solution and the required voltage is presented in Fig. 7b. The conductivity of the solution gradually increased from 0.930 to 5.572 mS/cm as the NaCl dosage was increased from 0.5 to 4.0 g/L. However, the voltage was observed to decrease from 14.85 to 4.05 V at lower NaCl dosages of 0.5 to 2.0 g/L before plateauing at higher NaCl dosages (3.0–4.0 g/L). Mouedhen et al. [40] suggested that the drop in the electrolysis voltage during the EC process could be caused by ohmic drop and/or decrease of overpotential in the anode. Therefore, 2.0 g/L was chosen as the best NaCl dosage based on the highest dye removal efficiency of almost 98.4% with a considerably lower voltage requirement. The results obtained in this present study were also in agreement with that reported in previous studies that 2.0 g/L was the optimum NaCl concentration required for the removals of Eriochrome Black [38] or Methylene blue [41] using aluminum electrodes.

3.2.5. Effect of inter-electrode distance

As the inter-electrode distance (IED) between the electrodes was increased at a constant current density, the electrical resistance increased, and consequently, the required voltage for the EC process also increased. Fig. 8a depicts the experimental results on the dye removal efficiency vs. time at different IEDs within the range of 0.5 to 2.5 cm. During the first 3 min of reaction, the dye removal efficiency noticeably decreased from 46.1% to 40.3% as the IED was increased from 0.5 to 2.5 cm. The reduction in the dye removal efficiency was due to lower collision between the Fe^{2+} ions and OH^- ions produced, as well as the longer time needed for these ions to react together (due to the longer distance to diffuse) [34]. Thus, this study suggested that different forms of oxygenated Fe could have been produced, whereby these forms of coagulants would be less

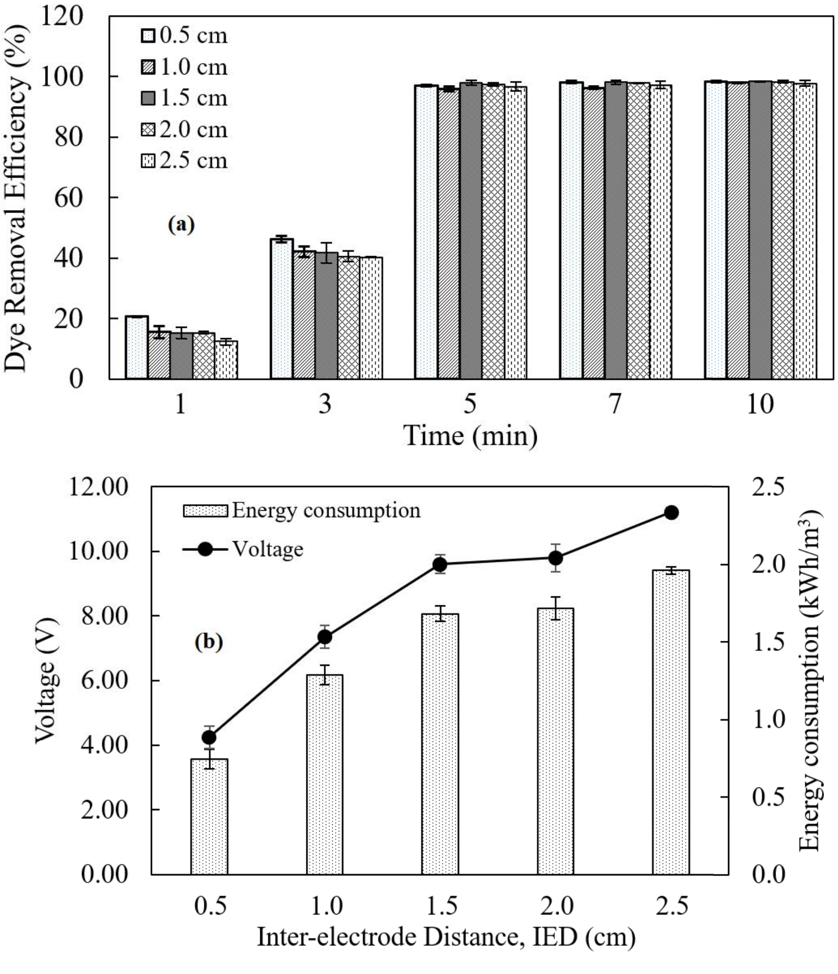

Fig. 8. Effects of inter-electrode distance on the (a) dye removal efficiency and (b) the voltage required and energy consumption during the electrocoagulation process by WSC electrode. (Current density = 10 mA/cm^2; initial pH = 6.8; initial dye concentration = 100 mg/L; NaCl = 2 g/L; time = 10 min).

active in the adsorption of the dye. However, after 5 min, the dye removal efficiencies obtained with all the IED were almost similar, that is, at around 97.0%. A further doubling of the reaction time to 10 min did not give any noticeable difference in terms of the dye removal performance.

Although the IED did not give much significant impact on the dye removal efficiency, an appropriate selection of IED was still crucial. This was based on the voltage required and consequently, the energy consumption for the EC process, especially when conductivity was low [34]. Fig. 8b presents the effect of IED on voltage and energy consumption during the EC process. The results revealed that as the IED was increased from 0.5 to 2.5 cm, the required voltage and energy consumption drastically increased from 4.25 to 11.2 V and 0.7439 to 1.9604 kWh/m^3, respectively. The increase in voltage could be attributed to an upsurge in electrical resistance as the IED was intensified at a constant current density. Therefore, the best operating IED selected during the EC process was 0.5 cm, whereby the energy consumption was minimized, with almost similar optimum values of IED reported in earlier studies using different electrodes [27,34].

3.3. Evaluation of the best-operating conditions on the decolorization of AR18 dye

From the parametric study, the best operating condition for decolorization of AR18 was identified to be at the current density of 10 mA/cm^2, a pH of 6.8 (original pH of dye), an initial dye concentration of 100 mg/L, a NaCl dosage of 2 g/L and an IED of 0.5 cm. The dye removal efficiency was observed to have reached up to 97.0% ± 1.0% in 5 min within these conditions, whereby the color of AR18 dye could be removed almost entirely at the end of the EC process. Further increase in the reaction time to 10 min was found to be unnecessary since the increment of dye removal efficiency was minimal (~1%–2%) or slightly reduced in certain cases. Additionally, the reaction time that was prolonged to more than 5 min observably caused the color of treated water to slightly change from being colorless to yellowish or brownish. It was due to the formation of minuscule iron ($Fe(OH)_3$ particles as suggested by Hussin et al. [25]. During the EC process, Fe^{2+} ions generated from anode oxidation could be easily oxidized to Fe^{3+} by dissolved oxygen that was present in the water. The minuscule Fe^{3+} ions were then transformed into yellowish $Fe(OH)_3$ particles that had poor stability.

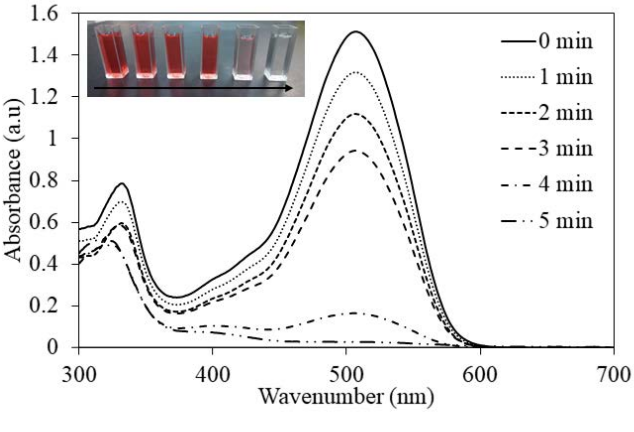

Fig. 9. Typical absorbance of AR18 dye during the EC process under the optimum conditions.

Table 1 shows the performances of using the EC process in removing AR18 dye as a comparison to the results reported by previous researchers. The dye removal efficiency observed in this study was found to be comparable with those reported in the literature. Interestingly, the electrodes derived from waste material as used in this study allowed the reaction to be carried out at the original pH of the dye in a relatively shorter reaction time. This finding could be of significant benefit to the EC process as the overall operating costs considering the electrode and energy consumption could be significantly reduced.

In this study, the removal of AR18 dye within 5 min of reaction could be further confirmed by the absorption spectrum as typically shown in Fig. 9. The absorption in the visible and UV regions was due to the presence of a chromophore group-containing azo linkage and aromatic (naphthalene) ring in the AR18 molecule. The electrocoagulation process was mainly thought to involve metal ion-induced agglomeration of dye substance to eventually settle or float as scum. As such, the conversion of dye molecules to other products or colorless intermediates could be minimum. The spectrum of AR18 dye exhibits two main peaks at 507 nm and 330 nm. The highest peak at 507 nm decreased significantly with time, which suggested that 5 min was sufficient to decolorize the dye almost completely through coagulation and adsorption mechanism at neutral pH [22,42]. Azarian et al. [18] reported a similar finding but at a relatively long reaction time of 30 min to achieve a complete decolorization of the same type of dye.

Meanwhile, the peak between 320 and 330 nm was observed to slowly decreased over time. This aromatic peak was reduced to only about 40% from the original absorbance, which indicated that some organic compounds present in the AR18 dye could not be entirely removed within 5 min of reaction time in this process. Buthiyappan et al. [43] also found that the aromatic compounds or other functional groups in their textile effluent were difficult to be removed due to the obstinate nature of wastewater, resulting in lower COD and total organic carbon removals even though a rapid decolorization was observed within the first 5 min of reaction. In contrast to this present study, Azarian et al. [18] reported that a similar peak between 320 and 330 nm of AR18 dye after the EC process appeared to be larger than the original peak to indicate the transition created during the EC process was also supported by lower COD removal. As both significant peaks (330 and 507 nm) decreased with time and no appearance of a new absorbance peak within the absorption spectrum, this study concluded that there was no significant presence of intermediate products that were created during the EC process using WSC electrodes.

The treated sample was also analyzed using ICP-OES to examine the Fe ions concentration that remained in the solution. This analysis was necessary to ensure that the EC using WSC electrodes was a safe process and no additional treatment was needed to manage the excessive residue of Fe ions after the process. From the results in Table 2,

Table 1
Comparison of AR18 dye removal using the EC process with some reported works

Electrode	Optimum operating conditions	Removal efficiency (%)	Reference
Al–Al	Current density: 26 mA/cm^2; pH: 4; reaction time: 40 min	92.3%	[30]
Fe–Fe	Current density: 1.2 mA/cm^2; pH: 7; reaction time: 45 min	99.5%	[15]
WSC/WSC	Current density: 10 mA/cm^2; pH: 6.8 (original pH of dye); reaction time: 5 min	97.0%	Present study

Table 2
Parameters of the EC process at the best-operating conditions

Parameter	Value
Dye removal, %	97.0 ± 1.0
[Fe], ppm remaining in the treated water	0.05
Final pH	7.82
Sludge produced (kg/m^3)	0.1164
EEC, (kWh/m^3)	0.3717
Operating cost, (US$/m^3 of wastewater)	0.9738

the residual Fe concentration in the treated water was found to be 0.05 ppm. Thus, WSC could be considered as effective electrodes, yet environmental friendly due to the low residual Fe concentration compared to the maximum allowable limit of 1.0 ppm for Standard A and 5.0 ppm for Standard B, as stated in the Fifth Schedule of Environmental Quality (Industrial Effluent) Regulation 2009 in Malaysia [44]. Furthermore, the final pH of the treated water was observed to be 7.82, which was also within the acceptable pH limit set for industrial effluent discharges.

Energy consumption during the EC process is also crucial and will contribute to the cost of operation. In this study, the energy consumption at the best-operating conditions was estimated to be at 0.3717 kWh/m^3. A similar range of energy consumption between 0.33 and 2.64 kWh/m^3 for the iron electrode at a reaction time between 15 to 45 min was reported by Azarian et al. [18]. Although the operating cost for treating synthetic dye wastewater was about US$0.9738/m^3, the operating cost obtained in this study was expected to be significantly lower as compared to the literature [28] due to the use of waste material as the electrodes, coupled with relatively shorter reaction time. Thus, the application of the WSC in the EC process was acceptable due to the high performance in removal efficiency. Based on economic considerations, the use of WSC also seemed to be industrially feasible.

3.4. Characterization analyses

The surface morphology and elemental composition of WSC floc generated from the EC process were examined using SEM-EDX analysis. Fig. 10a and b exhibit the surface morphology of WSC flocs at different magnifications of 500 x and 5000 x, respectively, while Fig. 10c shows the EDX results of the WSC flocs produced. Based on the results, the formed flocs exhibited non-uniformed shapes with micrometre-sized particles and could be characterized as having amorphous structures [22,45]. Based on the EDX analysis, the WSC floc contained a significant amount of Fe, at 52.34%, followed by 38.46% of O content. This result was due to the formation of $Fe(OH)_3$ as a coagulant that was mainly involved in the coagulation and adsorption of dye molecules on the coagulant surface owing to its large surface area [9]. The presence of C, with a composition of only 7.74%, was also expected because C was used as one of the alloying elements in the WSC packaging. In contrast, Na and Cl were present as NaCl was added into be the supporting electrolyte in increasing the conductivity of the solution. Meanwhile, 0.41% of the S component was also detected in the floc sample, owing to the electrostatic attraction of the negatively charged sulfonic group with the positively charged coagulant. This process further confirmed the occurrence of adsorption of dye molecules onto the generated flocs. A similar conclusion was reported by Mollah et al. [46], who assumed that the removal of Orange II dye was mainly caused by physisorption onto the floc surfaces through the presence of S, Al, Na, Cl and O components detected from EDX analysis.

Meanwhile, the IR spectra of the AR18 dye and WSC floc in the wavenumber that ranged between 4,000 to 400 cm^{-1} are shown in Fig. 11. The spectrum of AR18 dye exhibits a broad peak at 3,456 cm^{-1} due to the presence of O–H stretching vibration [22]. Meanwhile, the peak located at 1,635.64 cm^{-1} is attributed to the C=C of the aromatic ring [47]. The peaks occurring at 1,490.97 and 1,429.25 cm^{-1} are associated with the N=N stretching of the azo band and the C–N vibration of AR18 dye, respectively [22]. Meanwhile, the peaks detected at 1,190.08 and 1,047.35 cm^{-1} are due to the S=O bond of the sulfonic group [46].

Overall, the IR pattern of the parent AR18 dye could be retrieved from the WSC floc that was produced from the EC process. The vertical dotted lines showed similar peaks of WSC flocs with the parent dye. For the WSC floc, the O–H stretching vibrations appeared at 3,421.87 cm^{-1} while the small peak at 2,926.14 cm^{-1} was identified as C–H stretching. Additionally, the peak at 1,635.64 cm^{-1} recognized as the C=C vibration of the aromatic ring, alongside lower intensity peaks representing the N=N and C–N of the parent AR18 dye were also detected to confirm that the dye pollutant was adsorbed onto the flocs [22]. Meanwhile, the peaks at 1,192.06 and 1,026.17 cm^{-1} can be ascertained as the stretchings of S=O and C–O, whereby the S=O peak in the WSC floc appeared to resemble the parent AR18 dye. Besides, the peaks at around 1,192.06 and 559.38 cm^{-1} are also indicative of the formation of iron oxide hydroxide (FeO(OH)) and magnetite (Fe_3O_4), respectively [29]. These observations provided direct evidence to suggest

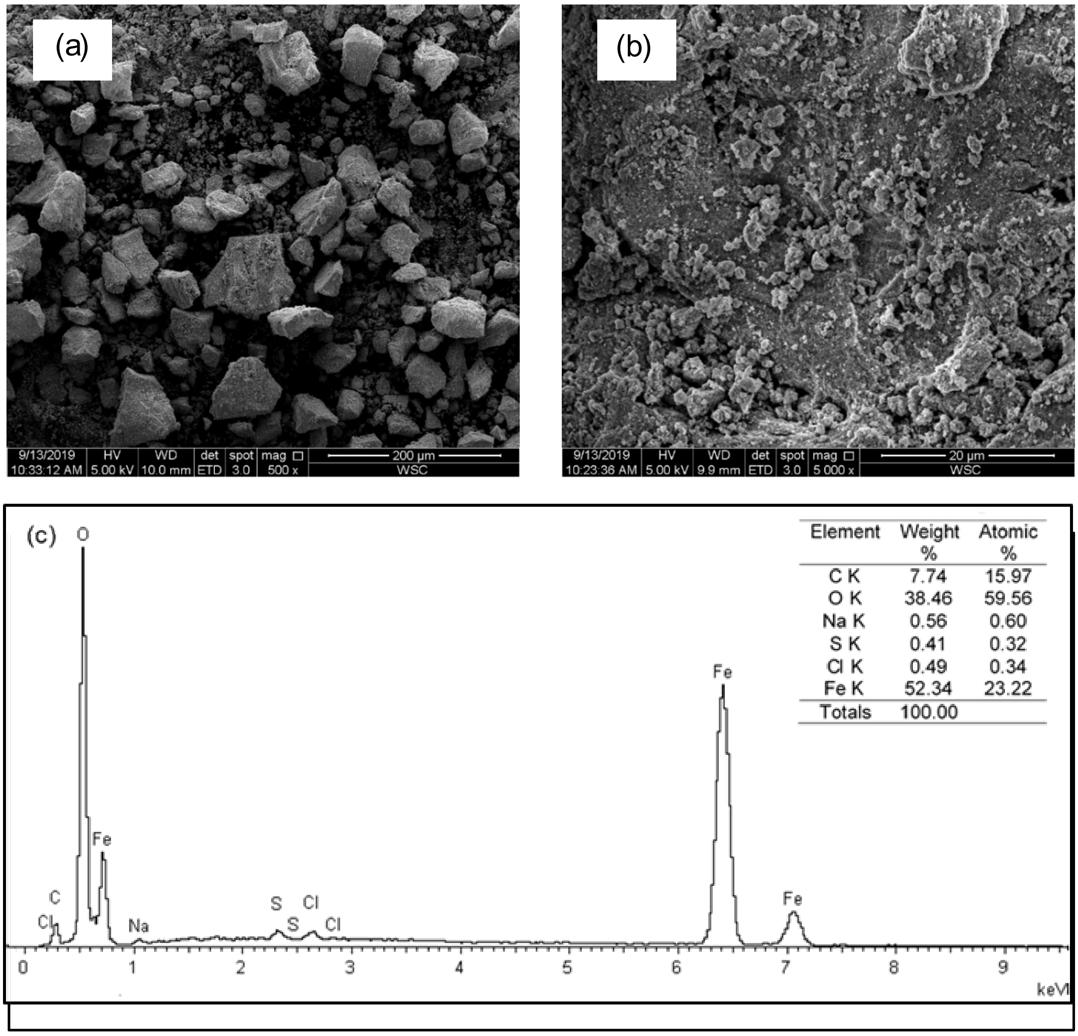

Element	Weight %	Atomic %
C K	7.74	15.97
O K	38.46	59.56
Na K	0.56	0.60
S K	0.41	0.32
Cl K	0.49	0.34
Fe K	52.34	23.22
Totals	100.00	

Fig. 10. SEM-EDX images of WSC flocs produced in the EC process at different magnifications (a) 500 x, (b) 5,000 x and (c) EDX analysis result.

that the primary mechanism in removing AR18 dye using WSC electrode was by coagulation and adsorption of the dye onto Fe flocs as reported in a previous study [11].

4. Conclusions

In this study, WSC was successfully transformed into efficient electrodes using simple mechanical pretreatment for the treatment of AR18 dye from aqueous solution through an EC process. Effects of the current density, initial pH, and concentration of dye, along with the contact time were demonstrated and the process behaviors were elucidated. Meanwhile, NaCl dosage and IED had significant influences on the voltage requirement of the process and should be taken into consideration towards minimizing energy consumption. The best-operating conditions were achieved at a current density of 10 mA/cm^2, a pH of 6.8 (original pH of dye), an initial dye concentration of 100 mg/L, a NaCl dosage of 2 g/L, an IED of 0.5 cm at only 5 min of process time. Under these conditions, energy consumption and operating cost were calculated

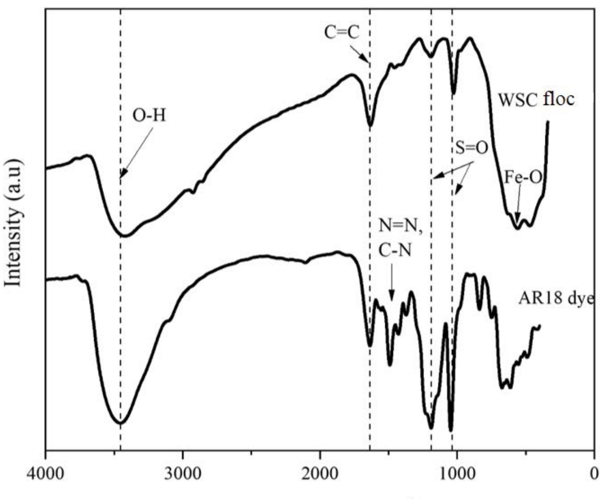

Fig. 11. Fourier-transform infrared spectrum of AR18 dye and WSC floc produced in the EC process.

to be 0.3717 kWh/m^3 and US$0.9738/$m^3$, respectively. The quality of the treated water was within the allowable limit for Malaysia's industrial effluent discharge standard. The residual Fe content in the water was only 0.05 ppm with a final pH of 7.82. The dominant pathway of dye removal was deemed to be through coagulation and adsorption of dye molecules onto the generated flocs.

Acknowledgments

The authors gratefully acknowledge the financial support from the Ministry of Higher Education of Malaysia for the LRGS grant (67215001) as well as Universiti Teknologi MARA (UiTM) for the postgraduate scholarship and study leave of the first author.

References

[1] M.M. Devi, K.N. Ojha, A.K. Ganguli, M. Jha, Transformation of waste tin-plated steel to iron nanosheets and their application in generation of oxygen, Int. J. Environ. Sci. Technol., 16 (2018) 3669–3678.

[2] National Solid Waste Management Department Malaysia, Survey on SW Composition, Characteristics & Existing Practice of SW Recycling in Malaysia, 2013. Available at: http://jpspn.kpkt.gov.my/resources/index/user_1/Sumber_Rujukan/kajian/Final_Report_REVz.pdf (accessed October 29, 2019).

[3] M.M. Devi, Sunaina, H. Singh, K. Kaur, A. Gupta, A. Das, S.T. Nishanthi, C. Bera, A.K. Ganguli, M. Jha, New approach for the transformation of metallic waste into nanostructured Fe_3O_4 and SnO_2-Fe_3O_4 heterostructure and their application in treatment of organic pollutant, Waste Manage., 87 (2019) 719–730.

[4] D.T. Moussa, M.H.E. Naas, M. Nasser, M.J.A. Marri, A comprehensive review of electrocoagulation for water treatment: potentials and challenges, J. Environ. Manage., 186 (2017) 24–41.

[5] S.O. Ganiyu, C.A.M. Huitle, M.A. Rodrigo, Renewable energies driven electrochemical wastewater/soil decontamination technologies: a critical review of fundamental concepts and applications, Appl. Catal., B, 270 (2020) 118857, doi: 10.1016/j.apcatb.2020.118857.

[6] S.O. Ganiyu, C.A.M. Huitle, The use of renewable energies driving electrochemical technologies for environmental applications, Curr. Opin. Electrochem., 22 (2020) 211–220.

[7] V. Khandegar, A.K. Saroha, Electrocoagulation for the treatment of textile industry effluent – a review, J. Environ. Manage., 128 (2013) 949–963.

[8] S.G. Segura, M.M.S.G. Eiband, J.V. de Melo, C.A.M. Huitle, Electrocoagulation and advanced electrocoagulation processes: a general review about the fundamentals, emerging applications and its association with other technologies, J. Electroanal. Chem., 801 (2017) 267–299.

[9] K. Gautam, S. Kumar, S. Kamsonlian, Decolourization of reactive dye from aqueous solution using electrocoagulation: kinetics and isothermal study, Z. Phys. Chem., 233 (2019) 1–22.

[10] C.A.M. Huitle, E. Brillas, Decontamination of wastewaters containing synthetic organic dyes by electrochemical methods: a general review, Appl. Catal., B, 87 (2009) 105–145.

[11] M. Chafi, B. Gourich, A.H. Essadki, C. Vial, A. Fabregat, Comparison of electrocoagulation using iron and aluminium electrodes with chemical coagulation for the removal of a highly soluble acid dye, Desalination, 281 (2011) 285–292.

[12] N.M.A. Ghalwa, A.M. Saqer, N.B. Farhat, Removal of reactive red 24 dye by clean electrocoagulation process using iron and aluminum electrodes, J. Chem. Eng. Process Technol., 7 (2016) 1–7.

[13] B.K. Nandi, S. Patel, Effects of operational parameters on the removal of brilliant green dye from aqueous solutions by electrocoagulation, Arabian J. Chem., 10 (2017) S2961–S2968.

[14] A.K. Verma, Treatment of textile wastewaters by electrocoagulation employing Fe-Al composite electrode, J. Water Process Eng., 20 (2017) 168–172.

[15] M. Malakootian, A. Moridi, Efficiency of electro-Fenton process in removing Acid Red 18 dye from aqueous solutions, Process Saf. Environ. Prot., 1 (2017) 138–147.

[16] E.H. Koupaie, M.R.A. Moghaddam, S.H. Hashemi, Post-treatment of anaerobically degraded azo dye Acid Red 18 using aerobic moving bed biofilm process: enhanced removal of aromatic amines, J. Hazard. Mater., 195 (2011) 147–154.

[17] E. Brillas, C.A.M. Huitle, Decontamination of wastewaters containing synthetic organic dyes by electrochemical methods. An updated review, Appl. Catal., B, 166–167 (2015) 603–643.

[18] G. Azarian, D. Nematollahi, A.R. Rahmani, K. Godini, M. Bazdar, H. Zolghadrnasab, Monopolar electro-coagulation process for azo dye C.I. Acid Red 18 removal from aqueous solutions, Avicenna J. Environ. Health. Eng., 1 (2014) 1–6.

[19] S.D. Cramer, B.S.J. Covino, ASM Handbook—Corrosion: Fundamentals, Testing, and Protection, 10th ed., ASM International, USA, 2003.

[20] A. Dura, C.B. Breslin, Electrocoagulation using stainless steel anodes: simultaneous removal of phosphates, Orange II and zinc ions, J. Hazard. Mater., 374 (2019) 152–158.

[21] N. Amri, A.Z. Abdullah, S. Ismail, Removal efficiency of Acid Red 18 dye from aqueous solution using different aluminium-based electrode materials by electrocoagulation process, Indones. J. Chem., 20 (2020) 536–544.

[22] P. Sakthisharmila, P.N. Palanisamy, P. Manikandan, Removal of benzidine based textile dye using different metal hydroxides generated in situ electrochemical treatment-a comparative study, J. Cleaner Prod., 172 (2018) 2206–2215.

[23] Tenaga Nasional Berhad Malaysia, Pricing & Tariffs, 2021. Available at: https://www.tnb.com.my/commercial-industrial/pricing-tariffs1/ (accessed January 19, 2021).

[24] M. Nasrullah, A.W. Zularisam, S. Krishnan, M. Sakinah, L. Singh, Y.W. Fen, High performance electrocoagulation process in treating palm oil mill effluent using high current intensity application, Chin. J. Chem. Eng., 27 (2019) 208–217.

[25] F. Hussin, F. Abnisa, G. Issabayeva, M.K. Aroua, Removal of lead by solar-photovoltaic electrocoagulation using novel perforated zinc electrode, J. Cleaner Prod., 147 (2017) 206–216.

[26] N.M. Niza, M.S. Yusof, M.A.A.M. Zainuri, M.I. Emmanuel, A.M.H. Shadi, M.A. Kamaruddin, Performance of batch electrocoagulation with vibration-induced electrode plates for landfill leachate treatment, J. Water Process Eng., 36 (2020) 101282, doi: 10.1016/j.jwpe.2020.101282.

[27] P. Ganesan, J. Lakshmi, G. Sozhan, S. Vasudevan, Removal of manganese from water by electrocoagulation: adsorption, kinetics and thermodynamic studies, Can. J. Chem. Eng., 91 (2013) 448–458.

[28] S. Bener, Ö. Bulca, B. Palas, G. Tekin, S.A. Atalay, G. Ersöz, Electrocoagulation process for the treatment of real textile wastewater: effect of operative conditions on the organic carbon removal and kinetic study, Process Saf. Environ. Prot., 129 (2019) 47–54.

[29] T. Kim, T.-K. Kim, K.D. Zoh, Removal mechanism of heavy metal (Cu, Ni, Zn, and Cr) in the presence of cyanide during electrocoagulation using Fe and Al electrodes, J. Water Process Eng., 33 (2020) 101109, doi: 10.1016/j.jwpe.2019.101109.

[30] A. Aleboyeh, N. Daneshvar, M.B. Kasiri, Optimization of C.I. Acid Red 14 azo dye removal by electrocoagulation batch process with response surface methodology, Chem. Eng. Process., 47 (2008) 827–832.

[31] C. Jiménez, C. Sáez, F. Martínez, P. Cañizares, M.A. Rodrigo, Electrochemical dosing of iron and aluminum in continuous processes: a key step to explain electro-coagulation processes, Sep. Purif. Technol., 98 (2012) 102–108.

[32] N. Liu, Y. Wu, Removal of Methylene blue by electrocoagulation: a study of the effect of operational parameters and mechanism, Ionics, 25 (2019) 3953–3960.

[33] K. Hendaoui, F. Ayari, I. Ben, R. Ben, F. Darragi, I.B. Rayana, R.B. Ammar, F. Darragi, M.T. Ayadi, Real indigo dyeing effluent decontamination using continuous electrocoagulation cell:

study and optimization using Response Surface Methodology, Process Saf. Environ. Prot., 116 (2018) 578–589.

[34] M.K. Mbacké, C. Kane, N.O. Diallo, C.M. Diop, F. Chauvet, M. Comtat, T. Tzedakis, Electrocoagulation process applied on pollutants treatment- experimental optimization and fundamental investigation of the crystal violet dye removal, J. Environ. Chem. Eng., 4 (2016) 4001–4011.

[35] R. Khosravi, S. Hazrati, M. Fazlzadeh, Decolorization of AR18 dye solution by electrocoagulation: sludge production and electrode loss in different current densities, Desal. Water Treat., 57 (2015) 1–9.

[36] I. Kabdaşli, B. Vardar, I.A. Alaton, O. Tünay, Effect of dye auxiliaries on color and COD removal from simulated reactive dyebath effluent by electrocoagulation, Chem. Eng. J., 148 (2009) 89–96.

[37] I. Kabdaşlı, I.A. Alaton, T.Ö. Hancı, O. Tünay, Electrocoagulation applications for industrial wastewaters: a critical review, Environ. Technol. Rev., 1 (2012) 2–45.

[38] D.T. Cestarolli, A. das Graças de Oliveira, E.M. Guerra, Removal of Eriochrome Black textile dye from aqueous solution by combined electrocoagulation–electroflotation methodology, Appl. Water Sci., 9 (2019) 1–5.

[39] E. Pajootan, M. Arami, N.M. Mahmoodi, Binary system dye removal by electrocoagulation from synthetic and real colored wastewaters, J. Taiwan Inst. Chem. Eng., 43 (2012) 282–290.

[40] G. Mouedhen, M. Feki, M.D.P. Wery, H.F. Ayedi, Behavior of aluminum electrodes in electrocoagulation process, J. Hazard. Mater., 150 (2008) 124–135.

[41] W. Pantorlao, D. Channei, W. Khanitchaidecha, A. Nakaruk, Decolorization of Methylene blue solution by electrocoagulation using aluminum electrodes, Chiang Mai J. Sci., 45 (2018) 2238–2243.

[42] A.R.A. Ghadim, S. Aber, A. Olad, H.A. Sorkhabi, Optimization of electrocoagulation process for removal of an azo dye using response surface methodology and investigation on the occurrence of destructive side reactions, Chem. Eng. Process. Process Intensif., 64 (2013) 68–78.

[43] A. Buthiyappan, A.A.A. Raman, W.M.A.W. Daud, Development of an advanced chemical oxidation wastewater treatment system for the batik industry, RSC Adv., 6 (2016) 25222–25241.

[44] Environmental Quality Act 1974 (Act 127), Regulations, Rules & Orders, International Law Book Services (ILBS), Malaysia, 2020.

[45] P.I. Omwene, M. Çelen, M.S. Öncel, M. Kobya, Arsenic removal from naturally arsenic contaminated ground water by packed-bed electrocoagulator using Al and Fe scrap anodes, Process Saf. Environ. Prot., 121 (2019) 20–31.

[46] M.Y.A. Mollah, J.A.G. Gomes, K.K. Das, D.L. Cocke, Electrochemical treatment of Orange II dye solution—use of aluminum sacrificial electrodes and floc characterization, J. Hazard. Mater., 174 (2010) 851–858.

[47] Y. Chen, B. Huang, M. Huang, B. Cai, On the preparation and characterization of activated carbon from mangosteen shell, J. Taiwan Inst. Chem. Eng., 42 (2011) 837–842.